Numerical investigation of titanium dioxide nanoparticles synthesis in laminar flames

J. M. Orlac'Ha, Nasser Darabiha, S Candel, Denis Veynante, Benedetta Franzelli

▶ **To cite this version:**

J. M. Orlac'Ha, Nasser Darabiha, S Candel, Denis Veynante, Benedetta Franzelli. Numerical investigation of titanium dioxide nanoparticles synthesis in laminar flames. 10th European Combustion Meeting (2021), Apr 2021, Napoli (virtual conference), Italy. hal-03407085

HAL Id: hal-03407085
https://hal.science/hal-03407085v1

Submitted on 29 Oct 2021

HAL is a multi-disciplinary open access archive for the deposit and dissemination of scientific research documents, whether they are published or not. The documents may come from teaching and research institutions in France or abroad, or from public or private research centers.

L'archive ouverte pluridisciplinaire **HAL**, est destinée au dépôt et à la diffusion de documents scientifiques de niveau recherche, publiés ou non, émanant des établissements d'enseignement et de recherche français ou étrangers, des laboratoires publics ou privés.

PROCEEDINGS VOLUME

www.ecm2021napoli.eu

Numerical investigation of titanium dioxide nanoparticles synthesis in laminar flames

J.M. Orlac'h[a], N. Darabiha[a], S. Candel[a], D. Veynante[a], B. Franzelli[a,*]

[a]*Laboratoire EM2C, Université Paris-Saclay, CNRS, CentraleSupélec, 1-3 rue du Joliot Curie, 91960 Gif-sur-Yvette, France*

Abstract

Production of titania nanoparticles from $TiCl_4$ precursor in 1-D laminar flames is investigated through numerical simulations. First, the impact of mass and enthalpy conservation in the modeling of nanoparticles production in reactive flows is investigated when considering high concentrations of particles precursor, classically characterizing the industrial applications. Then, a new model is developed accounting for a detailed description of $TiCl_4$ oxidation and a new hydrolysis pathway. Its performance is evaluated in premixed and non-premixed laminar configurations by comparison with state-of-the-art descriptions. Finally, TiO_2 production is characterized in both premixed and diffusion flames in terms of particle size Distributions (PSDs), in order to provide first indications on the optimization of TiO_2 flame synthesis.

1. Introduction

Flame processes are widely used for the manufacture of numerous nano-structured commodities, such as titanium dioxide – titania –, carbon black and fumed silica [1–4], representing a billion-dollar industry. Nanoparticle synthesis requires a fine control of the particle size and shape distributions, and of the nanoparticle crystal phase with desired properties depending on the targeted application. Therefore, detailed and accurate modelling of their production is of critical importance for the optimisation of nanoparticle production in flame reactors [5–7].

As a first step in this direction, it is important to derive and validate numerical models allowing a suitable representation of nanoparticles production in laminar flames. In the present work, we develop a full numerical strategy for the simulation of TiO_2 nanoparticles synthesis from titanium tetrachloride ($TiCl_4$) in laminar flames. This is done following three steps. First, the importance of a conservative formulation for mass and enthalpy in case of high nanoparticles concentration, as in practical flame synthesis applications, is discussed in Section 3. Second, the importance of accounting for hydrolysis in detailed kinetics of $TiCl_4$ consumption to reproduce a fast and efficient conversion rate, in agreement with experimental evidences, is discussed in Section 4. Finally,TiO_2 production in laminar flames is analyzed in Section 5 in terms of particle size distribution to provide some indications on the optimisation of flame synthesis systems.

2. Physical models

In the following, TiO_2 production from $TiCl_4$ synthesis in 1-D laminar premixed and non-premixed counterflow methane/air flames will be investigated using the Regath code [8]. Also, 2-D simulations of a coflow methane/air flame will be performed using the LaminarSmoke code [9, 10].

2.1. Gas phase description and $TiCl_4$ consumption

Two main approaches can be found in the literature to describe TiO_2 flame synthesis from $TiCl_4$ consumption:

- Global fitted descriptions: Among them, the global model due to Pratsinis et al. [11] has been developed to describe $TiCl_4$ consumption:

$$TiCl_4(g) + O_2(g) \rightarrow TiO_2(s) + 2Cl_2(g). \quad (1)$$

The reaction follows an Arrenhius formulation. Even if the mechanism is presented in the form of a one-step oxidation reaction, the rate is first-order with respect to $TiCl_4$ and zeroth-order in O_2, meaning that it does not depend on O_2 concentration. The rate constants of the global reaction have been fitted to provide a reasonable estimation of the experimental global $TiCl_4$ consumption [11, 12] and it is at the heart of many numerical studies of TiO_2 nanoparticles formation [12–17]. This model has been recently validated on a laminar coflow diffusion flame and reproduced reasonably well the nanoparticles volume fraction and particle size distributions [18].

- Detailed oxidation kinetics: a detailed mechanism for the gas-phase reactions of $TiCl_4$ with O_2 has been first developed by West et al. [19] based on density functional theory (DFT) calculations to be consistent with thermodynamic equilibrium theory. It accounts for 30 species and 66 reactions. This detailed model was shown in [20] to agree reasonably well with the global description in terms of $TiCl_4$ consumption rate [21, 22]. However, to our knowledge, a detailed mechanism of this type has not been validated in terms of nanoparticle volume fraction or number density. In addition, the detailed mechanism has mostly been applied to $TiCl_4$-O_2 mixtures heated externally[21–23]. This corresponds to water free configurations that are not necessarily representative of nanoparticles production in flames, where the presence of water may induce $TiCl_4$ hydrolysis and require a description of this process to correctly predict TiO_2 production. Additional detailed oxidation kinetics [20, 24], presenting similar features and performances, have been developed from this scheme.

*Corresponding author: benedetta.franzelli@centralesupelec.fr

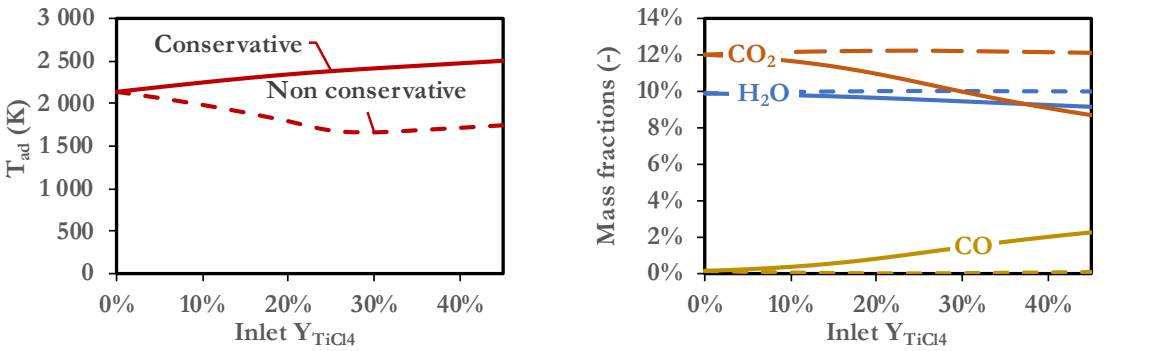

a) b)

Figure 1: a) Equilibrium temperature and b) combustion product mass fractions as a function of inlet TiCl4 mass fraction in thermodynamic equilibrium calculations. Results with the conservative and non-conservative formulations are represented in continuous and dashed lines, respectively.

From this literature survey, it appears that global descriptions can be considered as a good approach for the prediction of TiO_2 production in flames (i.e. $TiCl_4$ consumption, conversion yield, and lognormal particle size distribution,PSD) since they have been specifically fitted for it. However, as for all global chemical models, they do not provide any realistic kinetics information. On the contrary, the detailed oxidation models can be considered as good models for the prediction of TiO_2 production when it occurs through $TiCl_4$ oxidation. However, it may fail when considering flame synthesis if hydrolysis is not negligible.

In the present work, the global model from Pratsinis [11] and the detailed oxidation mechanism from Mehta et al. [24] are considered. This detailed mechanism accounts for 36 species, 15 quasi-steady-state species and 237 reactions. It comprises three blocks: methane oxidation, chlorination of methane and Ti oxidation, based on the detailed scheme by West et al.[19]. For the sake of consistency, when working with the global model, the gaseous phase is described by the the subset of the detailed scheme relevant to methane combustion by removing Ti- and Cl-containing species.

2.2. *Solid phase description*

The solid phase is conveniently described with a sectional model providing an accurate representation of the particle size distribution. The particles diffusion velocity involves a thermophoretic contribution [25, 26] and a diffusion term induced by concentration gradients. The particles diffusion coefficients are computed in the free molecular regime. The particle thermophoresis velocity is taken from Waldmann [25]. Particle production is characterized by the conversion of $TiCl_4$ precursor molecule into solid particles containing from several tens to thousands of Ti atoms. The nanoparticles dynamics involve nucleation and coagulation. The coagulation rate is expressed in a transition regime between the free molecular and the continuum regime [27]. In general, the nucleated particles are treated as monomers [12]. Here, following the recommandations of Mehta et al. [28], we consider the freshly nucleated particles to contain five Ti atoms.

3. Importance of mass and enthalpy conservation

When considering the operating conditions correspondent to industrial applications, the conservation of the total enthalpy and/or the total mass may become critical. Indeed, in most models, when the particle volume fraction is very small, particle enthalpy exchange and differential diffusion are neglected. However, TiO_2 nanoparticles synthesis in flames is usually characterized by a high conversion rate and, consequently, a high concentration in nanoparticles that may reach up to 50% in terms of mass fraction.

As the purpose of this section is essentially to demonstrate the importance of using a conservative set of equations, the global scheme is adopted here. In order to highlight the importance of a conservative formulation in terms of enthalpy [27], thermodynamic equilibrium calculations are carried out. The considered fresh gas composition corresponds to an equivalence ratio $\phi = 0.8$, a fresh gas temperature of T=500 K and a pressure of P=1 bar, with an increasing concentration of $TiCl_4$.

When the $TiCl_4$ inlet concentration is increased, the

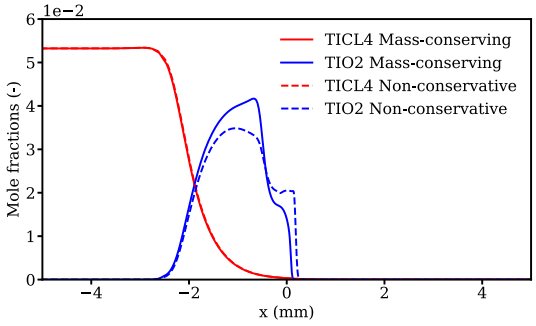

Figure 2: $TiCl_4$ and TiO_2 mole fraction profiles for a 1D counterflow CH_4/O_2 flame. The inlet temperature is 500 K. Injected $TiCl_4$ mass fraction $Y^{inj}_{TiCl_4} = 0.25$ at the oxidizer side. Strain rate $\alpha = 600\,s^{-1}$. The stagnation plane is located at $x = 0$ mm. Comparison between the mass-conserving (continuous lines) and the non-conservative (dashed lines) formulations.

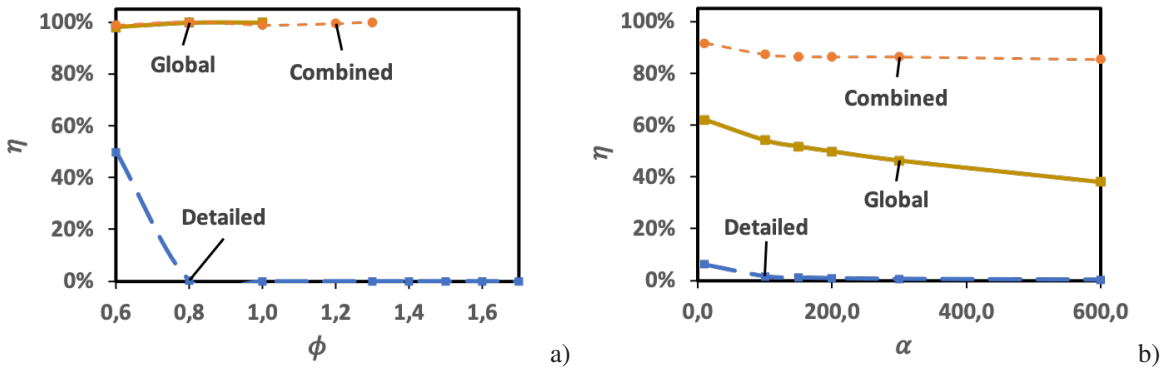

Figure 3: Conversion yield as a function of a) equivalence ratio and b) strain rate in 1D premixed and diffusion flames, respectively. Inlet $TiCl_4$ mass fraction $Y^{\text{inj}}_{\text{TiCl}_4} = 0.05$. Comparison among three kinetics.

effect of a conservative formulation is made evident, as can be seen on Fig. 1a, where the equilibrium temperatures corresponding to both model formulations are compared. When the inlet $TiCl_4$ mass fraction is 25%, the equilibrium temperature with a non-conservative formulation is lowered down to 1681 K, which represents a relative error of roughly 30%. This demonstrates the importance of enthalpy conservation when high nanoparticles mass fractions are involved.

The effect on the species mass fractions is also significant, as can be seen in Fig. 1b. As soon as the mass fraction of $TiCl_4$ reaches 10%, relative errors on the titanium containing species range from 20% to 100% (not shown). The relative errors in CO_2, H_2O, and CO mass fractions can be respectively of the order of 45, 10, and 95%. In addition to the errors on species mass fractions and temperature, it is observed that using a non-enthalpy-conserving formulation may lead to severe numerical difficulties.

The importance of differential diffusion is also investigated considering a 1D counterflow flame. Even though the particles diffuse slower than the gaseous species, the conservation of mass requires to account for a correction velocity due to thermophoresis. Contrary to enthalpy conservation, no numerical instabilities are observed due to non-conservation of mass. Yet, the formulation of the diffusion velocities has an important impact on the titania mass fraction profiles, presented in Fig. 2, with almost 15% relative error, though a marginal impact on the flame structure (not shown). The use of a conservative formulation for mass and enthalpy is then mandatory when considering high nanoparticles concentrations.

4. Accounting for both oxidation and hydrolysis of $TiCL_4$

As already indicated, among the different models available in literature, one finds on the one hand global models that are fitted to retrieve global quantities (such as $TiCl_4$ consumption rate), but do not provide insight into the actual nucleation kinetics. On the other hand, detailed thermodynamically-consistent oxidation schemes have been derived under dry conditions and still require additional validation for flame synthesis, where $TiCl_4$ hydrolysis may be the dominant nucleation pathway due to the presence of water vapour (H_2O) generated by combustion.

To improve their accuracy for nanoparticle flame synthesis, a new model combining a detailed oxidation kinetics with a recently-developed kinetic mechanism for hydrolysis has been proposed [29]. The performances of the global scheme from Pratsinis, the detailed oxidation model from Mehta and the recent combined oxidation/hydrolysis models are evaluated in what follows.

First, 1-D premixed methane/air flames at different equivalence ratio is considered (inlet temperature T=500 K, inlet $TiCl_4$ mass fraction $Y_{TiCl_4^{inj}} = 0.05$ and atmospheric pressure). The conversion yield as a function of the equivalence ratio is plotted for the three chemical schemes in Fig. 3a. As the rate constant of the global model is of order 0 in O_2, this model is not adapted to the simulation of rich flames. Therefore for the global model only lean conditions are considered. It can be seen that for all equivalence ratios ϕ both the global model and the combined oxidation/hydrolysis kinetics lead to nearly 100% conversion. For both schemes, the conversion yield is thus independent of ϕ, so that the equivalence ratio has no impact on the final volume fraction of particles. On the contrary, the detailed oxidation kinetics does not seem to predict a fast conversion of $TiCl_4$ into TiO_2 a result that is at variance with experimental evidences [30, 31]. The corresponding conversion yield is significant only when the equivalence ratio ϕ is lower than 0.6, and is negligible for higher equivalence ratios. The addition of the hydrolysis kinetics to the detailed oxidation kinetics appears therefore as necessary to correctly reproduce the fast conversion rate.

Second, 1-D counterflow methane/air flames are now considered for different values of the strain rate α, where $TiCl_4$ is injected on the oxidizer side with a mass fraction equal to 5%. The conversion yield in the counterflow flame is plotted as a function of the strain rate α for the three schemes in Fig. 3b. For all schemes, the conversion yield is a decreasing function of the strain rate, as increasing the strain rate lowers the residence time in the flame. For all strain rates, the combined oxidation/hydrolysis scheme leads to a higher conversion rate than the global model, itself leading to a much higher rate than the detailed oxidation scheme. As in the premixed flame, the

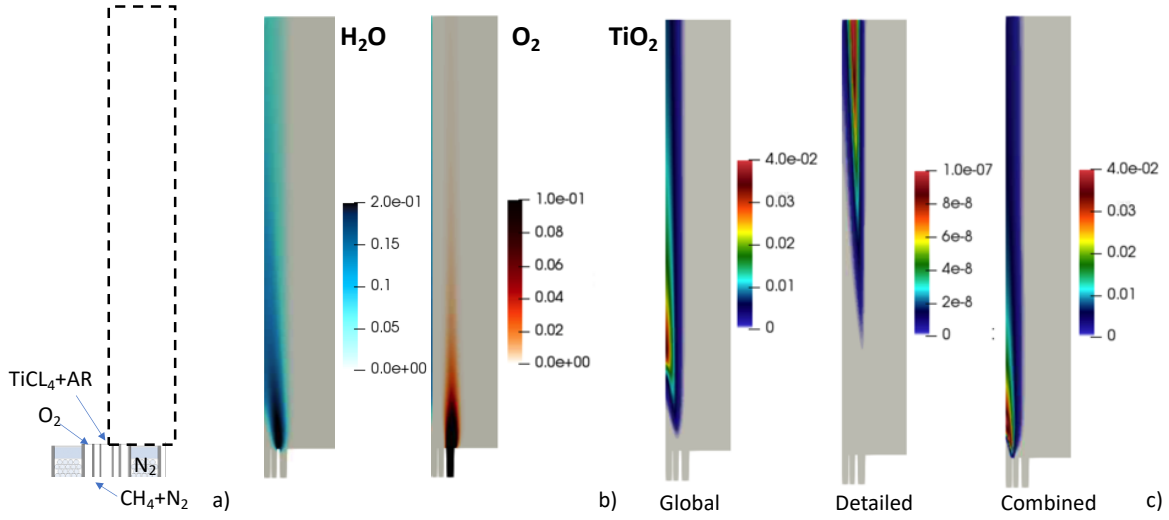

Figure 4: a) TiO_2 production in a coflow flame ($Y^{inj}_{TiCl_4} = 0.25$). b)O_2 and H_2O mass fractions are visualized to identify the oxidation and hydrolysis zones. c) The TiO_2 mass fraction is obtained with a global model, a detailed oxidation and the newly developed combined oxidation/hydrolysis kinetics.

detailed oxidation model does not predict a fast conversion of $TiCl_4$ into TiO_2, in contrast with previous experimental evidences in diffusion flames [30, 31]. Compared to the premixed flame, none of the proposed kinetics predicts full conversion in the counterflow flame. Additionally, the global model, which is known to be fast, predicts lower conversion rates than the combined scheme including hydrolysis, with conversion yield even below 40% at 600 s^{-1}. While the yield is nearly independent on strain rate when $\alpha \leq 100$ s^{-1} for the combined scheme, for the global model the yield is a markedly decreasing function of strain rate. This is due to the fact that the combined scheme is extremely fast so that it is less sensitive to the residence time.

Finally, the performances of the three model are evaluated on a 2-D coflow methane/air flame[18], schematically represented in Fig. 4a. It should be noticed that the global oxidation model provides a reasonable agreement with experiments in this configuration [18]. Two-dimensional fields of O_2 and H_2O mass fractions are illustrated in Fig. 4b to identify regions where oxidation and hydrolysis of $TiCl_4$ may occur. It can be observed in Fig. 4c that the global and the newly-developped models predict a fast TiO_2 production along the centerline close to the injector. On the contrary, the detailed oxidation model is characterized by a slow TiO_2 production, so that an inefficient coefficient rate is observed, similarly to results on 1-D premixed and non-premixed flames. By examining to O_2 and H_2O fields, it may be deduced that the $TiCl_4$ will experience hydrolysis and will convert into TiO_2 before encountering O_2.

These results suggest than that $TiCl_4$ hydrolysis is a major contributor to TiO_2 formation in flames, due to the presence of water vapor and the high reactivity of $TiCl_4$ with vapor. It is therefore essential to account for this process in a detailed kinetics scheme.

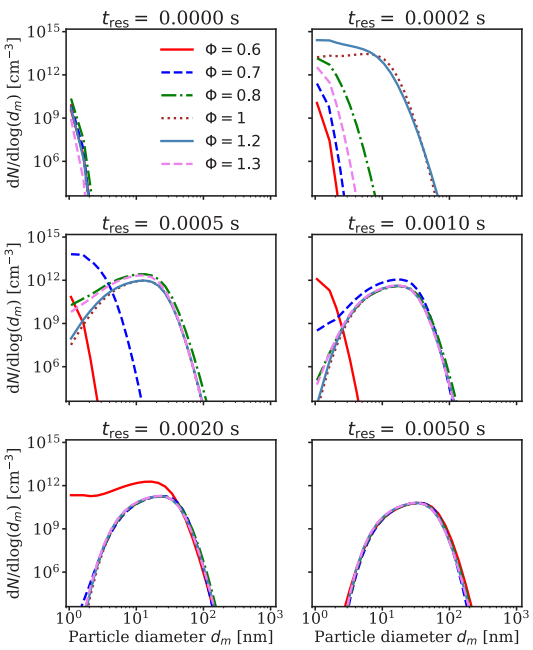

Figure 5: Particle Size Distribution (PSD) at different residence times in a premixed flame for different values of equivalence ratio ϕ using the combined mechanism.

5. Investigation of titanium dioxide flame synthesis

Finally, TiO_2 synthesis in flames is investigated for 1-D premixed and non-premixed flames in terms of Particle Size Distribution (PSD). In premixed flames, the PSDs are observed to depend only on the nanoparticle lifetimes t_{res}, regardless of the equivalence ratio. Indeed, it can be seen in Fig. 5 that the PSDs corresponding to all equivalence ratios superimpose on the same curve: after only 5 ms, the same lognormal distribution is attained for almost all equivalence ratios. However, the transient evolutions towards the lognormal distribution do not coincide. In particular, the closer to the stoichiometric conditions,

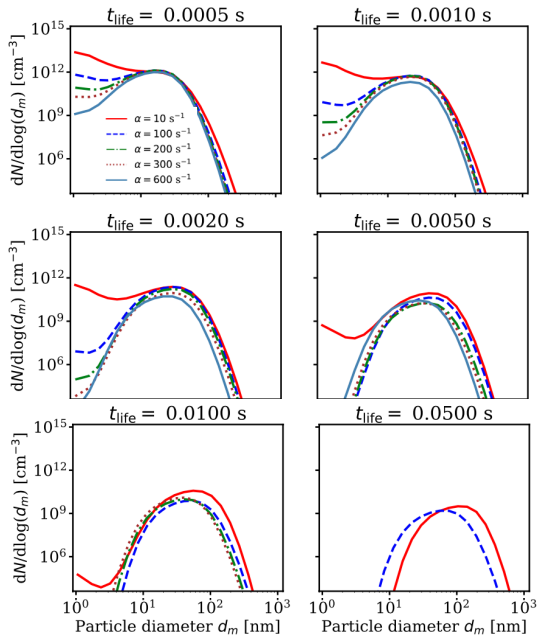

Figure 6: Particle Size Distribution (PSD) at different residence times in a counterflow diffusion flame for different values of the strain rate α using the combined kinetics.

the faster the lognormal distribution is attained. This is likely so because of higher temperature and H_2O mass fraction at stoichiometric conditions. Similarly, the precursor concentration do not significatly modify the PSD (not shown), even if the case with highest concentration induces a higher average diameter and a larger standard deviation for a given residence time.

In non-premixed counterflow flames, the PSDs maily depend on nanoparticle lifetimes too (Fig. 6), but the flame structure is more complex, and thermophoresis influences the volume fraction profile (not shown). Therefore, longer residence times (more than 50 ms) are needed to retrieve a lognormal distribution. As expected, a final lognormal distribution is observed both in premixed and non-premixed flames (cfr Fig. 7a). In the premixed flame, the non-dimensional number density function, NDF, superimposes on the same universal distribution, presented in Fig. 7b. On the contrary, in the non-premixed flames they are close to each other but do not perfectly superimpose perfectly since shorter residence times characterize this kind of configuration.

6. Conclusion

The production of titania nanoparticles from flame synthesis has been investigated by developing a numerical strategy for TiO_2 production using $TiCl_4$ as precursor. First, the importance of a conservative formulation in terms of mass and enthalpy to correctly predict temperature and species mass fractions has been discussed for classical laminar flame configurations. It is then shown that detailed kinetics developed in dry configurations and accounting only for $TiCl_4$ oxidation are characterized by extremely long TiO2 formation time scales and, consequently, by low conversion yields when applied in flame configurations. These results are in contrast with the experimental evidences and the numerical results predicted by a global fitted model, showing an efficient and fast process for TiO_2 formation by flame synthesis. A more general detailed kinetics is proposed by complementing the oxidation kinetics with a recently-developed hydrolysis kinetics. The combined kinetics is able to retrieve the behavior expected for TiO_2 production in flame while providing access to detailed chemical pathways. These results suggest that $TiCl_4$ hydrolysis is a major contributor to TiO_2 nucleation in flames, due to the presence of water vapor and the high reactivity of $TiCl_4$ with vapor.

Finally, TiO_2 synthesis in 1-D laminar flames has been characterized in terms of PSD. In general, it can be stated that the PSDs rapidly take a lognormal shape, regardless of the equivalence ratio for premixed flames and strain rate for non-premixed flames. The residence time is a key parameter in the PSD evolution. Therefore, in the premixed flame, the non-dimensional NDF superimposes on the same universal distribution, while in the non-premixed flames they are close to each other but do not perfectly coincide since shorter residence times characterize this kind of configuration.

Acknowledgments

This work has received funding from the European Research Council (ERC) under the European Union Horizon 2020 research and innovation programme (grant agreement No. 757912).

References

[1] E. Pratsinis, Prog. Energy Combust. Sci. 23 (1998) 197–219.
[2] Z. Xu, H. Zhao, Combustion and Flame 162 (2015) 2200–2213.
[3] G. A. Kelesidis, E. Goudeli, S. E. Pratsinis, Proceedings of the Combustion Institute 36 (2017) 29–50.
[4] C. Schulz, T. Dreier, M. Fikri, H. Wiggers, Proceedings of the Combustion Institute (2018).
[5] C. Weise, A. Faccinetto, S. Kluge, T. Kasper, H. Wiggers, C. Schulz, I. Wlokas, A. Kempf, Combustion Theory and Modelling 17 (2013) 504–521.
[6] V. Raman, R. O. Fox, Annual Review of Fluid Mechanics 48 (2016) 159–190.
[7] J. Sellmann, I. Rahinov, S. Kluge, H. Jünger, A. Fomin, S. Cheskis, C. Schulz, H. Wiggers, A. Kempf, I. Wlokas, Proceedings of the Combustion Institute (2018).
[8] P. Rodrigues, B. Franzelli, R. Vicquelin, O. Gicquel, N. Darabiha, Proceedings of the Combustion Institute 36 (2017) 927–934.
[9] A. Cuoci, A. Frassoldati, T. Faravelli, E. Ranzi, Energy & Fuels 27 (2013) 7730–7753.
[10] A. Cuoci, A. Frassoldati, T. Faravelli, E. Ranzi, Combust. Flame 160 (2013) 870–886.
[11] S. E. Pratsinis, H. Bai, P. Biswas, M. Frenklach, S. V. R. Mastrangelo, Journal of the American Ceramic Society 73 (1990) 2158–2162.
[12] S. E. Pratsinis, P. T. Spicer, Chemical Engineering Science 53 (1998) 1861–1868.
[13] Y. Xiong, M. Kamal Akhtar, S. E. Pratsinis, Journal of Aerosol Science 24 (1993) 301–313.
[14] P. T. Spicer, O. Chaoul, S. Tsantilis, S. E. Pratsinis, Journal of Aerosol Science 33 (2002) 17–34.
[15] S. Tsantilis, S. E. Pratsinis, Journal of Aerosol Science 35 (2004) 405–420.
[16] N. Morgan, C. Wells, M. Goodson, M. Kraft, W. Wagner, Journal of Computational Physics 211 (2006) 638–658.
[17] M. C. Heine, S. E. Pratsinis, Particle & Particle Systems Characterization 24 (2007) 56–65.
[18] Z. Xu, H. Zhao, H. Zhao, Proceedings of the Combustion Institute 36 (2017) 1099–1108.
[19] R. H. West, M. S. Celnik, O. R. Inderwildi, M. Kraft, G. J. O. Beran, W. H. Green, Industrial & Engineering Chemistry Research 46 (2007) 6147–6156.

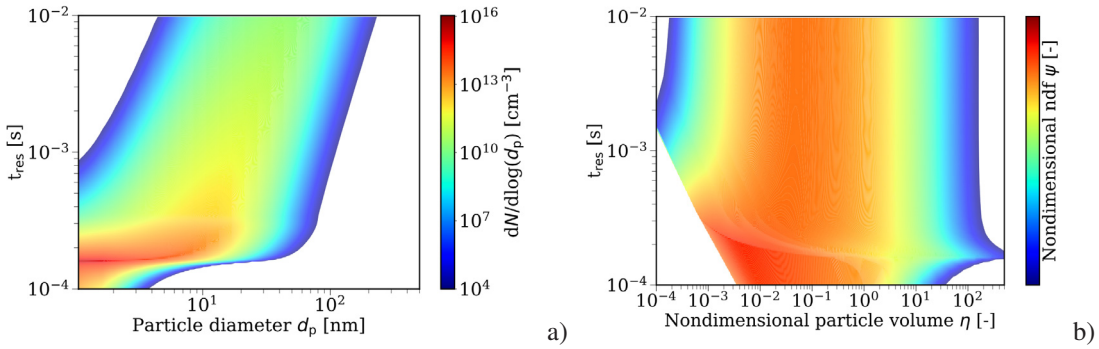

Figure 7: a) Particle Size Distribution and b)Non-dimensional Number Density Function in a premixed flame using the combined kinetics.

[20] R. H. West, R. A. Shirley, M. Kraft, C. F. Goldsmith, W. H. Green, Combustion and Flame 156 (2009) 1764–1770.

[21] J. Akroyd, A. J. Smith, R. Shirley, L. R. McGlashan, M. Kraft, Chemical Engineering Science 66 (2011) 3792–3805.

[22] C. Lindberg, J. Akroyd, M. Kraft, Chemical Engineering Science 166 (2017) 53–65.

[23] A. Boje, J. Akroyd, S. Sutcliffe, J. Edwards, M. Kraft, Chemical Engineering Science 164 (2017) 219–231.

[24] M. Mehta, R. O. Fox, P. Pepiot, Industrial & Engineering Chemistry Research 54 (2015) 5407–5415.

[25] L. Waldmann, K. Schmitt, in: Aerosol Science, Academic Press, New York, davies, c. n. edition, 1966, pp. 137–162.

[26] B. V. Derjaguin, A. I. Storozhilova, Y. I. Rabinovich, Journal of Colloid and Interface Science 21 (1966) 35–58.

[27] J.-M. Orlac'h, N. Darabiha, V. Giovangigli, B. Franzelli, Combust. Theory Modelling (2021).

[28] M. Mehta, Y. Sung, V. Raman, R. O. Fox, Industrial & Engineering Chemistry Research 49 (2010) 10663–10673.

[29] J.-M. Orlac'h, N. Darabiha, S. Candel, D. Veynante, B. Franzelli, Modeling of titania nanoparticle production from ticl4 in 1d-premixed and counterflow laminar flames, In progress.

[30] L.-D. Chen, W. Roquemore, Combustion and Flame 66 (1986) 81–86.

[31] W. Zhu, S. E. Pratsinis, in: G.-M. Chow, K. E. Gonsalves (Eds.), Nanotechnology, volume 622 of *ACS Symposium Series*, American Chemical Society, Washington, DC, 1996, pp. 64–78.